01 Mar 2014

Porous Titania Microspheres with Uniform Wall Thickness and High Photoactivity

Xinhua Liang
Missouri University of Science and Technology, liangxin@mst.edu

Rajankumar L. Patel

Recommended Citation

X. Liang and R. L. Patel, "Porous Titania Microspheres with Uniform Wall Thickness and High Photoactivity," *Ceramics International*, vol. 40, no. 2, pp. 3097 - 3103, Elsevier, Mar 2014.
The definitive version is available at https://doi.org/10.1016/j.ceramint.2013.10.001

Available online at www.sciencedirect.com

ScienceDirect

Ceramics International 40 (2014) 3097–3103

CERAMICS INTERNATIONAL

www.elsevier.com/locate/ceramint

Porous titania microspheres with uniform wall thickness and high photoactivity

Xinhua Liang*, Rajankumar L. Patel

Department of Chemical and Biochemical Engineering, Missouri University of Science and Technology, Rolla, MO 65409, USA

Received 26 July 2013; received in revised form 28 September 2013; accepted 1 October 2013
Available online 8 October 2013

Abstract

Highly porous titania particles were prepared by depositing thin films of titania, using alternating reactions of $TiCl_4$ and hydrogen peroxide, on poly(styrene-divinylbenzene) (PS-DVB) template particles via atomic layer deposition (ALD) at 77 °C. The composition of the titania films was verified by XPS analysis and the titania films were directly observed by TEM. TGA/DSC was used to study the thermal decomposition of the polymer template. Porous titania particles with uniform wall thicknesses were successfully obtained after the template PS-DVB was removed by oxidation in air at 400 °C for 24 h. Verification of the resulting porous structure of the titania particles was done by cross-sectional SEM and nitrogen adsorption–desorption analysis. Porous titania particles were treated at different temperatures. XRD analysis was used to determine the microstructure and phase transformation of titania at elevated temperatures. The photocatalytic activity of these porous titania particles was studied by methylene blue decomposition under UV light at room temperature and was found to be comparable to that of commercial anatase titania nanoparticles (~20 nm). Depositing Na_2SO_4 on TiO_2 retarded the TiO_2 phase transformation from anatase to rutile during calcination and, thus, greatly increased the photoactivity of the porous titania particles.

Keywords: Atomic layer deposition (ALD); Coating; Titania; Porous; Photoactivity

1. Introduction

Titania (TiO_2) is extensively studied for use in different applications including dye-sensitized solar cells [1], hydrocarbon and hydrogen production [2–5], and CO_2 reduction [6–8], because of its high photoactivity, chemical stability, non-toxicity, and low cost [9]. Titania has a band gap energy of 3–3.2 eV. Under UV light, the energy of a photon is equal to or greater than the band gap energy of titania, and electron–hole pairs can be created in the transition of the excited electrons from valance band to conduction band [9]. This creates hydroxyl radicals as a result of oxidation–reduction reactions that occur on the surface of each particle. Hydroxyl groups and oxygen radicals play an important role in the decomposition of organic compounds on the surfaces of titania particles. Detailed information on the photocatalytic process has been covered in several review articles [9,10].

To increase the efficient usage of titania, high surface area titania nanoparticles are normally used. However, the smaller the particle size, the more difficult it is to separate titania nanoparticles from the reaction system for their re-use. This problem could be readily solved if we used large porous titania particles that had high surface areas. The high photocatalytic activity of these particles can be retained because of their high surface areas, since large particle sizes make recovery and re-use much simplier. These highly porous titania particles can be easily applied to a continuous flow reactor for water treatment or other photocatalytic processes, essentially making the whole system easy to handle and more eco-friendly by recovering the titania particles and reusing them.

A number of articles have been published that document the preparation of titania microspheres. Many techniques have been developed to synthesize meso-microporous titania using facile template methods, such as chemical implantation [11], a sol–precipitation method [12–14], the templating of polymers [15–17], or hydrothermal synthesis [18]. For example, Zhong et al. prepared hollow spheres of TiO_2 by using a sol–gel precursor solution on a crystalline array of a polystyrene

*Corresponding author. Tel.: +1 5 73341 7632.
E-mail address: liangxin@mst.edu (X. Liang).

0272-8842/$ - see front matter © 2013 Elsevier Ltd and Techna Group S.r.l. All rights reserved.
http://dx.doi.org/10.1016/j.ceramint.2013.10.001

template [13]. Lin et al. successfully developed porous nanocrystalline TiO_2 photocatalysts using a sol–gel technique with polyethylene glycol as the structure directing agent [14]. Sun et al. used carbonaceous polysaccharide microspheres as templates for the fabrication of hollow spheres of titania [17]. Recently, some novel methods have been developed to self-formulate template-free hollow titania materials using continuous spray pyrolysis [19], and a spontaneous self-formation procedure [20], among others [21]. These methods provide different ways of preparing TiO_2 hollow spheres. However, in many cases there are issues with the ability to control the microstructural and morphological of the synthesized particles [10], and there is no control over the wall thicknesses of the titania porous structures. This study provides an alternative to these methods by preparing porous titania particles that have uniform wall thicknesses through the use of atomic layer deposition (ALD).

ALD is a layer-by-layer gas phase deposition technique [22–24]. It provides highly uniform and conformal coating of metal oxides on 3-D structures due to alternating self-limiting saturative surface reactions. The deposition of ALD films can be controlled to a 0.1 nm range. This gives a commanding lead over the control provided by other techniques. Ultra-thin titania films that are deposited via ALD at low temperatures (< 100 °C) are amorphous [25,26] and have low photoactivity [26]. Heat treatment, however, can enhance the photoactivity of titania. In this study, we used ALD to deposit titania films (with thicknesses that could be controlled) onto a porous polymer template. Porous titania particles were formed after the polymer template was removed. The porous structure of these particles and the influence of calcination treatment on the phase structures were determined by using various techniques, including SEM, XRD, and nitrogen adsorption and desorption. The photoactivity of the titania particles were studied by methylene blue decomposition under UV light.

2. Experimental

2.1. ALD of titania films

Porous poly(styrene-divinylbenzene) (PS-DVB) particles were synthesized by the copolymerization of styrene and divinylbenzene [27]. The size of the particles was ~450 μm (Fig. 1), with a porosity of ~80%, a bulk density of ~0.07 g/cm^3, and a surface area of 42 m^2/g. The titania ALD coating process was carried out in a fluidized bed reactor, which was similar to the one previously described in detail [28]. The fluidized bed system consisted of a reactor column, a vibration generation system, a gas flow control system, and a data acquisition and control system with LabView®. High-purity nitrogen gas was used as the fluidization gas and purge gas. The flow of nitrogen gas was maintained using a mass flow controller from MKS Instruments. All valves used to provide the transient dosing were automatically controlled by LabView® and pressure measurements were recorded to monitor the progress of each dosing cycle. The system was operated at reduced pressures. $TiCl_4$ (ReagentPlus®, 99.9% trace metals basis, Sigma Aldrich) and concentrated H_2O_2 (30–32 wt% in water, semiconductor grade, 99.999% trace metals basis, Sigma Aldrich) were used as reactants for TiO_2 ALD at 77 °C. Since corrosive HCl is one of the byproducts, a liquid nitrogen cold trap was connected to the inlet of the vacuum pump to condense the HCl byproduct. One gram of porous polymer particles was loaded into the reactor and the minimum pressure was ~10 Pa inside the reactor. The minimum fluidization superficial gas velocity was 0.8 cm/s. Precursors were fed separately through the distributor plate at the base of the reactor using their room-temperature vapor pressures as the driving force. A typical coating cycle used the following sequence: $TiCl_4$ dose (180 s), N_2 purge (1200 s), evacuation (120 s); H_2O_2 dose (240 s), N_2 purge (1200 s), evacuation (120 s). 200 cycles of titania ALD were applied.

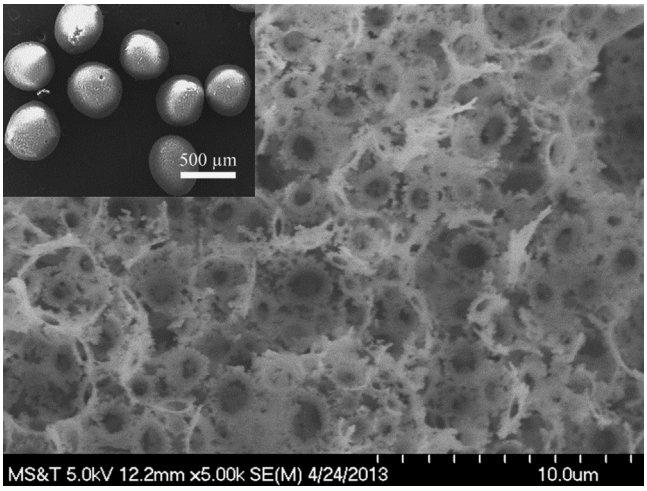

Fig. 1. Cross-sectional SEM image of PS-DVB porous particles. The inset image shows the size of the PS-DVB particles.

2.2. Formation of titania microspheres

To remove the organic constituent after ALD, the titania-coated PS–DVB particles were heated in air at 400 °C for 24 h. Almost all of the organic constituent had been removed, since the particles were white after oxidation. To study the phase transition and thermal stability of titania nanoparticles, calcination was also conducted at 600 °C and 800 °C for an additional 2 h, at a heating rate of 10 °C/min. It was reported that depositing Na_2SO_4 on TiO_2 could significantly retard the TiO_2 phase transformation from anatase to rutile during calcination at elevated temperatures [29]. To obtain sulfated TiO_2 (TiO_2–SO_4^{2-}) with 1 wt% of SO_4^{2-}, the porous titania particles obtained at 400 °C were soaked in a certain amount of Na_2SO_4 solution, air dried, and then calcined at 800 °C for 2 h.

2.3. Characterization

X-ray photoelectron spectroscopy (XPS) (Kratos Axis 165) was used to verify the composition of titania films by employing Al K (a) excitation, operated at 150 W and 15 kV. The coated PS-DVB particles were visualized with an FEI Tecnai F20 field emission gun high resolution TEM/STEM equipped with an energy dispersive X-ray spectrometer

(EDX) system, which allowed the elemental analysis of samples while imaging. TEM samples were prepared by placing the crushed porous particles on holey-carbon films supported on Cu grids. The porous polymer and titania particles were studied using a Hitachi S-4700 Field Emission Scanning Electron Microscope. The cross-sectioned specimens were prepared by cutting the particles using a Super Gillette blue blade. At least three spots per sample were analyzed by STEM and FESEM. Thermo-gravimetric analysis of the titania-coated polymer particles was conducted using a Netzsch TGA/DTA with a flowing air atmosphere (50 mL/min) at a heating rate of 2 °C/min, up to 1000 °C. A Quantachrome Autosorb-1 was used to obtain nitrogen adsorption and desorption isotherms of the ALD-coated particles before and after oxidation in air at -196 °C. Before starting the adsorption measurements, each sample was outgassed at 120 °C for 12 h. The specific surface areas of the samples were calculated using the Brunauer–Emmett–Teller (BET) method in a relative pressure range of 0.05–0.25. The total pore volumes were calculated from the adsorption quantity at a relative pressure of $P/P_0 = 0.99$. The pore size distribution curves were derived from the desorption branches of the isotherms using the Barrett–Joyner–Halenda (BJH) method. The XRD analysis was performed using PANanalyticalX'pert MPD instrument and copper target with Kα radiation of 1.5418 Å (λ). Samples were analyzed at 40 mA current and 45 kV tension of X-ray generator at 1.4°/min scan rate.

2.4. Photoactivity test

Aqueous methylene blue (MB) solution was used to evaluate the photoactivity of porous titania particles. For comparison, the photoactivity of the commercial anatase titania nanoparticles (~20 nm) and of the P-25 titania particles was also tested. Each time, 0.1 g of sample was dispersed in a 100 mL, 10 ppm MB solution. Previous work [26,30] indicated that the equilibrium of adsorption–desorption in the solution could be achieved in 60 min for all of the prepared samples. A 100 W UV lamp was used for 360 nm UV irradiation at a distance of 10 cm from the surface of the solution. This distance ensured that the UV light intensity would be ~10 mW/cm^2, as confirmed from the previous work [26,30]. At certain time intervals, 2 mL test samples were taken from the main solution and filtered through a 0.2 μm Millipore filter to make it particle-free for analysis using an UV–vis spectrometer (Varian Cary 50-Bio) at a 664 nm wavelength. The change in concentration of MB in the main solution was recorded over a period of irradiation time.

3. Results and discussion

XPS measurements were obtained for uncoated and titania-coated porous PS-DVB particles after 200 ALD cycles. In Fig. 2, the spectrum for the uncoated porous polymer particles showed a strong C 1 s photoelectron peak at 284.7 eV. In contrast, the carbon spectrum for coated particles revealed a much weaker photoelectron intensity at 284.7 eV. The reduction of

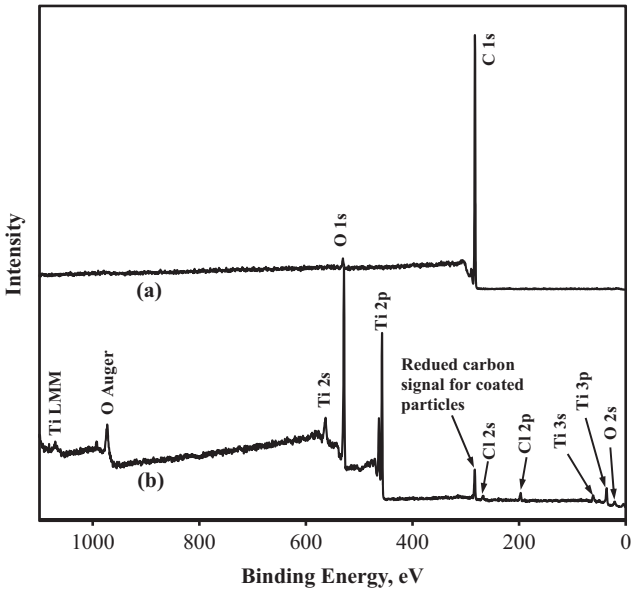

Fig. 2. XPS spectra of (a) uncoated and (b) TiO_2-coated porous polymer particles after 200 cycles.

the C signal was expected since the titania films conformally covered the entire porous polymer particle surface. However, the carbon XPS signal could not be completely attenuated as some of the carbon signal corresponded to surface carbon. Photoelectrons from the titania-coated particles were observed at 565.2 eV (Ti, 2 s), 458.7 eV (Ti, 2p), and 530.0 eV (O, 1 s), which clearly confirmed the presence of TiO_2. A small amount of chlorine was the residual from the precursor, which was removed during the heat treatment process that followed [31].

The titania-coated porous polymer particles were analyzed by using STEM. A representative STEM image of the titania-coated polymer particles, after 200 ALD cycles, is shown in Fig. 3. The regions with a brighter contrast were titania films. Clearly, the titania films grown on the internal and external polymer particle surfaces appeared to be very smooth. The thickness of the titania films was ~40 nm, which represented a growth rate of 0.2 nm per coating cycle. This growth rate was much higher than previously reported results that also used $TiCl_4$ and concentrated H_2O_2 as precursors. The growth rate of titania ALD on PS-DVB, at 100 °C, was reported to be ~0.06 nm per coating cycle [32]. Similar results were reported for titania ALD on silicon wafers at 100 °C [31]. The much higher growth rate in this study could be explained by the lower reaction temperature (77 °C). It is well known that the growth rate of titania ALD films is highly dependent on the reaction temperatures, and the surface coverage of reactants will increase at lower temperatures. Although the reaction kinetics is slower at lower temperatures, the growth rate is determined by the higher surface coverage [33,34]. This kind of higher growth rate on polymer substrates has been observed for other ALD thin films [27,28], since thin film ALD on polymers is normally carried out at lower temperatures. On the other hand, it would be much more difficult to remove the excess water or peroxide from porous particles at lower

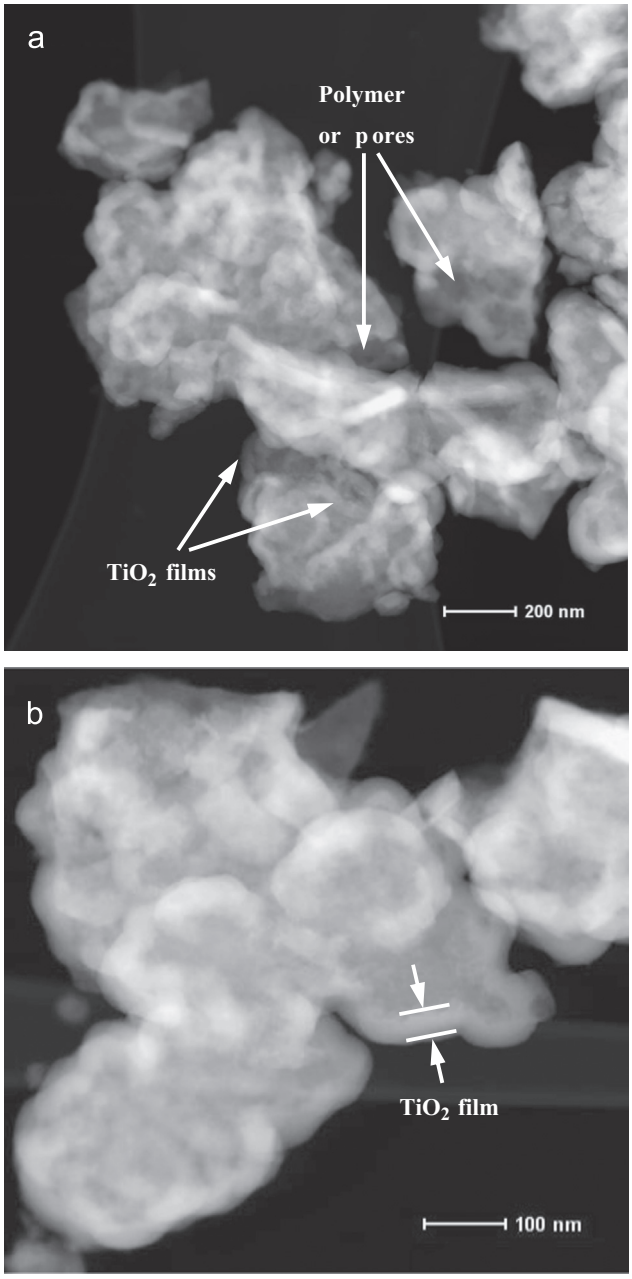

Fig. 3. (a and b) STEM images of 200 cycles of titania ALD-coated PS–DVB particles.

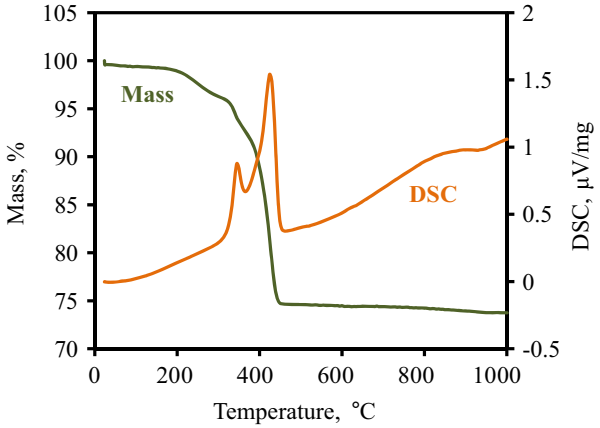

Fig. 4. TGA and DSC curves of 200 cycles of titania ALD-coated PS-DVB particles measured at a heating rate of 2 °C/min.

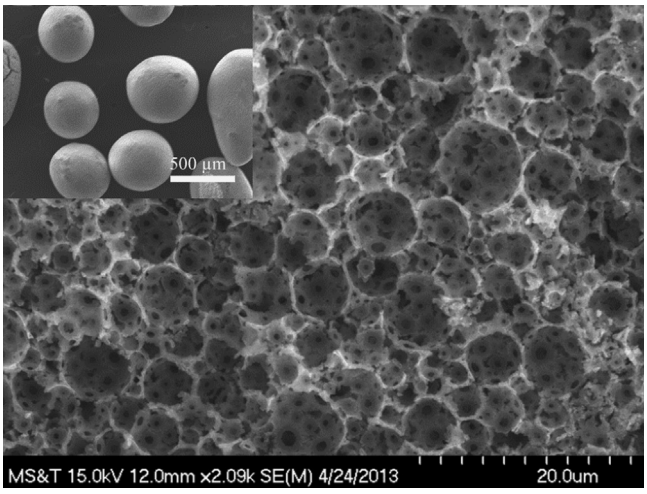

Fig. 5. Cross-sectional SEM image of titania porous particles. The inset image shows the size of the titania particles.

temperatures, even though the inter-gas flush time in this study was very long. In this case, a local CVD could happen, which would contribute to the higher film growth rate. After 200 cycles of titania ALD, the surface area of the polymer particles was 8.1 m^2/g, compared to the surface area of 42 m^2/g for the uncoated particles. This reduction was due to the filling of the pores with titania ALD films.

The results of the thermo-gravimetric analysis of the titania-coated polymer particles are shown in Fig. 4. The heating rate was 2 °C/min. The main mass loss began at 200 °C, and no mass loss was observed when the temperature was above 450 °C. The total mass loss was about 26%, which means the polymer particles composed about 74% of titania after 200 cycles of titania ALD coating. During the decomposition of PS–DVB, the organic component was released as CO_2 and H_2O and porous titania structures formed. Fig. 4 also shows a DSC curve of 200 cycles of titania ALD coated PS–DVB particles. Obviously, there is one crystallization peak centered at 420 °C, indicating the transformation of amorphous titania to anatase titania. With the removal of the organic component, the resulting porous titania particles maintained the shape and the morphology of the polymer templates, as shown in the inset image in Fig. 5. The porous structure was maintained after the removal of the polymer template. The macropores were three-dimensionally packed and interconnected, but the structure of the titania was more rigid than that of the porous polymer, as shown in Fig. 5.

The porous structure of the titania particles was studied further by using nitrogen adsorption and desorption analysis. Fig. 6 shows the nitrogen adsorption and desorption isotherms, surface area, pore volume, and pore size distributions of porous titania particles fabricated from 200 cycles of titania ALD-coated polymer particles after being oxidized or calcined

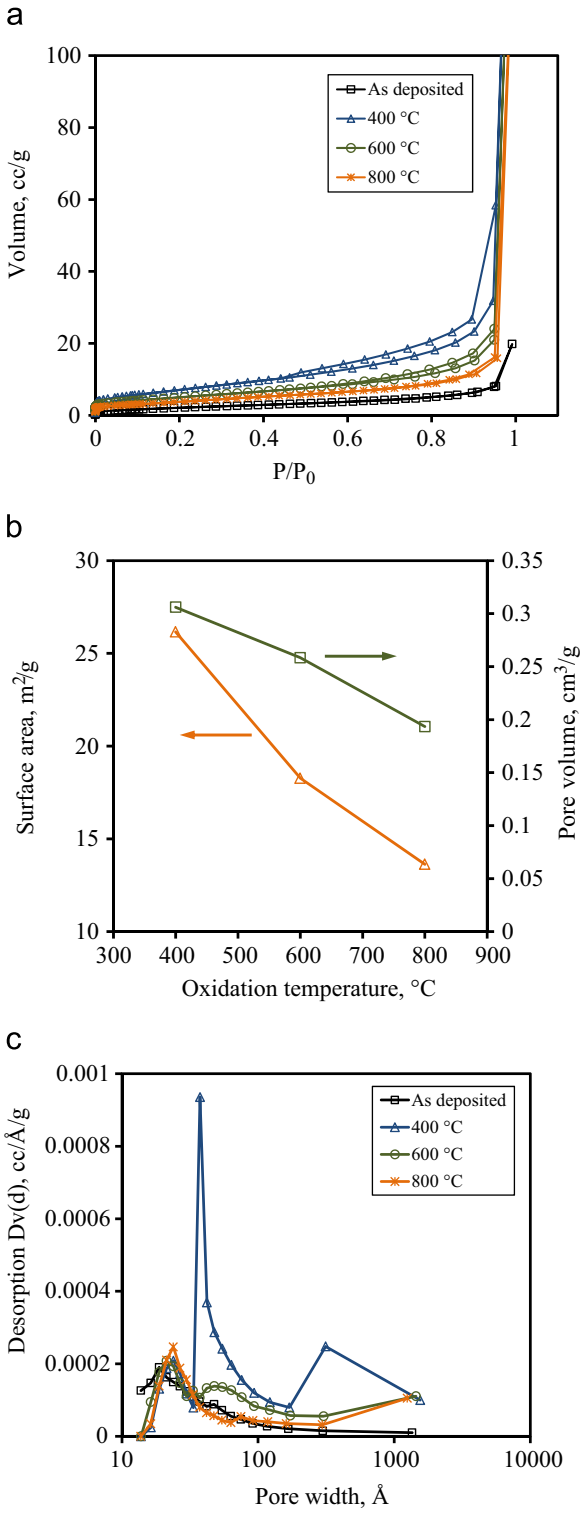

Fig. 6. (a) Nitrogen adsorption and desorption isotherms, (b) surface area and pore volume, and (c) pore size distributions of porous titania particles fabricated from 200 cycles of titania ALD-coated polymer particles oxidized at different temperatures.

at different temperatures. After oxidation in air at 400 °C for 24 h, most of the organic component was removed, and the surface area of the porous particles had greatly increased to 26.2 m^2/g, as compared to the surface area of 8.1 m^2/g for titania ALD-coated polymer particles before oxidation. Correspondingly, the pore volume of the particles increased from 0.03 cm^3/g for the as-deposited particles to 0.31 cm^3/g for the particles after the removal of the organic component. Part of the surface area could have resulted from the formation of some sub-nano sized pores, due to the release of gaseous by-products that formed porous nano-structures, since the polymer component was sandwiched between two layers of titania ALD films. As shown in Fig. 6c, after the removal of the polymer component at 400 °C, the number of micropores, mesopores, and macropores greatly increased, as compared to the as-coated polymer particles. The pore size distribution was wide, in the range of 1–120 nm. With an additional 2 h of calcination at 600 °C, or 800 °C, both the surface areas and the pore volumes of the particles decreased. For example, the surface area and pore volume of the particles were 13.6 m^2/g and 0.19 cm^3/g, respectively, after heated in air at 800 °C. This reduction was most likely due to the collapse of the micropores in the frameworks during the heat treatment process. The transformation of anatase to rutile destroyed some of the micropores in the frameworks.

A titania structure undergoes phase transformation from anatase to rutile at elevated temperatures [35], so the effects of heat treatment on the phase structures of titania were studied by XRD. Fig. 7 shows the varied XRD patterns of titania-coated PS-DVB particles before and after heat treatment at different temperatures. It can be seen that the as-deposited titania-coated PS-DVB particles have no crystal structure.

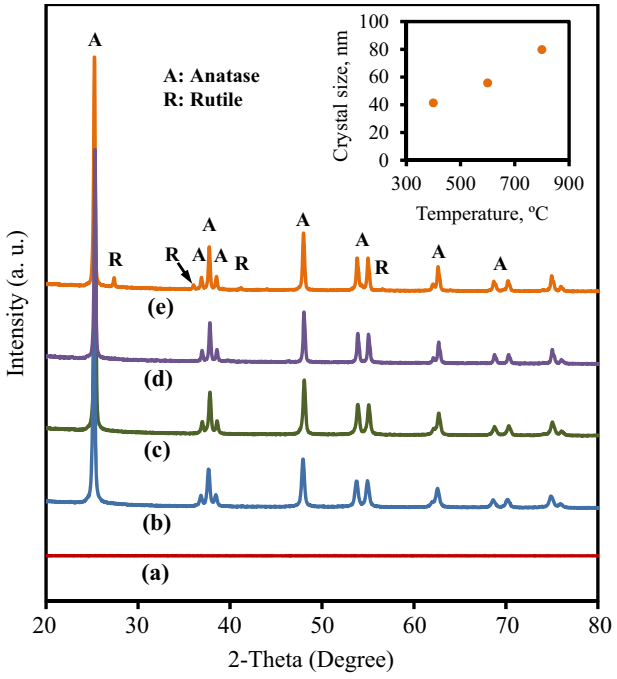

Fig. 7. XRD patterns of (a) as-deposited 200 cycles of titania-coated PS-DVB particles, (b) 200 cycles of titania-coated PS-DVB particles oxidized in air at 400 °C for 24 h, (c) sample b heated in air at 600 °C for an additional 2 h, (d) 1% SO_4^{2-} in sample b after heated in air at 800 °C for an additional 2 h, and (e) sample b heated in air at 800 °C for an additional 2 h. The inset figure shows the titania crystal size increase with the increase in treatment temperature.

The anatase phase of the titania particles was seen after the removal of the polymer template in air at 400 °C for 24 h, but there was no sign of a rutile structure. There was no phase transition from anatase to rutile after calcination of the particles in air at 600 °C for 2 h, but it was evident when the titania particles were treated in air at 800 °C for 2 h. There was no noticeable rutile phase for the sulfated TiO_2 (TiO_2–SO_4^{2-}) with 1 wt% of SO_4^{2-} heated in air at 800 °C for 2 h. Depositing Na_2SO_4 on TiO_2 retarded the TiO_2 phase transformation from anatase to rutile during calcination [29]. The XRD reflections of anatase and rutile phase became narrower with increases in temperature, which indicated a growth in crystal sizes in that particular phase. Assuming that the titania had spherical nanostructures, the crystal sizes (L) were calculated using the Scherrer equation [36]:

$$\beta = \frac{0.94\lambda}{L\cos\theta}$$

where θ is the diffraction angle of the most intense peak which occurs at about 25 °C for all samples, β is the peak width at half maximum after subtracting the instrumental broadening. The inset figure in Fig. 7 shows that the anatase titania crystal size increased with the increase in treatment temperature, which agreed with the previous report [37–39]. The average crystallite size of samples treated at 400 °C and 600 °C increased slowly, from 43.2 to 58.2 nm, and then jumped to 83.2 nm at 800 °C. Heat treatment temperatures can affect crystal sizes proportionally and, also, above 700 °C the phase transformation occurs from anatase to rutile [37]. This phase transformation can help explain the results from the surface areas and the pore volumes shown in Fig. 6. As discussed earlier, the surface areas and the pore volumes decreased with increases in the calcination temperature.

The photocatalytic activity of the fabricated porous titania particles was evaluated by the degradation of MB in an aqueous solution. As shown in Fig. 8, the effectiveness of these porous titania particles was compared with the commercial anatase titania particles (~20 nm size) and commercial P-25 titania particles that contain both the anatase and rutile phases. The relative concentration of MB was zero in 90 min for all of the samples tested. The photocatalytic activity of titania particles, obtained by oxidation of titania coated PS-DVB particles at 400 °C, was very similar to that of the commercial anatase particles. The photoactivity of the porous titania, with an additional 2 h heat treatment at 800 °C, was comparable to that of the commercial P-25. The sulfated TiO_2 (TiO_2–SO_4^{2-}) with 1 wt% of SO_4^{2-}, after heat treatment at 800 °C for 2 h, had the highest photocatalytic degradation efficiency. When the anatase titania was calcinated at 800 °C, it achieved higher crystallinity and the number of defects was reduced, which increased the photoactivity. Also, heat treatment at 800 °C caused the phase transformation from anatase to rutile. The conversion of anatase to rutile decreased the photoactivity, since rutile titania has lower photoactivity than that of anatase titania. Depositing Na_2SO_4 on TiO_2 retarded the TiO_2 phase transformation from anatase to rutile during calcination, and the photoactivity of the porous titania particles was greatly increased. Both the phase composition and the high crystallinity of TiO_2 contributed to the high photoactivity of the titania particles.

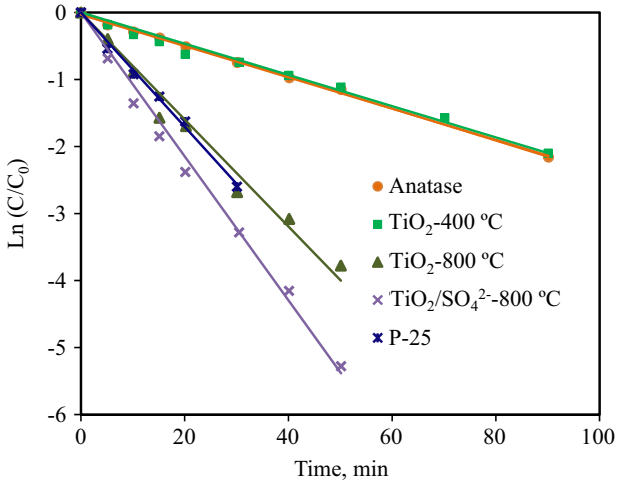

Fig. 8. Methylene blue concentration in photocatalytic tests as a function of UV irradiation time: (a) ~20 nm commercial anatase titania particles, (b) porous titania particles obtained by oxidation of PS-DVB particles coated with 200 cycles of titania ALD in air at 400 °C, (c) sample from (b) oxidation in air at 800 °C for an additional 2 h, (d) 1% SO_4^{2-} in sample after oxidation in air at 800 °C for an additional 2 h, and (e) commercial P-25 titania particles.

4. Conclusions

Titania films were deposited on porous PS-DVB particles using ALD. The template polymer was removed by oxidation in air and the remaining titania porous particles maintained the shape and the morphology of the PS-DVB template. SEM images confirmed that the titania particles were free standing and highly porous. N_2 absorption studies further verified the interconnected porous structure of the titania particles. The photocatalytic activity of these porous titania particles was studied by methylene blue decomposition under UV light at room temperature. The photoactivity of the porous titania was comparable to that of the commercial anatase titania nanoparticles. Depositing Na_2SO_4 on TiO_2 retarded the TiO_2 phase transformation from anatase to rutile during calcination and, thus, greatly increased the photoactivity of the porous titania particles. This study indicates that highly porous titania particles, with controllable wall thicknesses, could be prepared via an ALD template-directed process. These microspheres with high photoactivity could be used in a fixed bed reactor for water treatment and the large particle size could make them much easier to recover and re-use.

Acknowledgments

This work was partly supported by the Materials Research Center at the Missouri University of Science and Technology. The author thanks Dr. Kai Song and Brian Porter at the Materials Research Center for the TEM analysis and the XPS analysis, respectively.

References

[1] M. Paulose, K. Shankar, O.K. Varghese, G.K. Mor, C.A. Grimes, Application of highly-ordered TiO_2 nanotube-arrays in heterojunction dye-sensitized solar cells, Journal of Physics D-Applied Physics 39 (2006) 2498–2503.

[2] S.S. Tan, L. Zou, E. Hu, Photocatalytic production of methane and hydrogen through reduction of carbon dioxide with water using titania pellets, International Journal of Green Energy 3 (2006) 283–290.

[3] H. Yoshida, K. Hirao, J.I. Nishimoto, K. Shimura, S. Kato, H. Itoh, T. Hattori, Hydrogen production from methane and water on platinum loaded titanium oxide photocatalysts, The Journal of Physical Chemistry C 112 (2008) 5542–5551.

[4] G.L. Chiarello, M.H. Aguirre, E. Selli, Hydrogen production by photocatalytic steam reforming of methanol on noble metal-modified TiO_2, Journal of Catalysis 273 (2010) 182–190.

[5] S. Mozia, A. Heciak, A.W. Morawski, Photocatalytic acetic acid decomposition leading to the production of hydrocarbons and hydrogen on Fe-modified TiO_2, Catalysis Today 161 (2011) 189–195.

[6] K. Adachi, K. Ohta, T. Mizuno, Photocatalytic reduction of carbon-dioxide to hydrocarbon using copper-loaded titanium-dioxide, Solar Energy 53 (1994) 187–190.

[7] M. Anpo, H. Yamashita, Y. Ichihashi, S. Ehara, Photocatalytic reduction of CO_2 with H_2O on various titanium oxide catalysts, Journal of Electroanalytical Chemistry 396 (1995) 21–26.

[8] C.-C. Lo, C.-H. Hung, C.-S. Yuan, Y.-L. Hung, Parameter effects and reaction pathways of photoreduction of CO_2 over TiO_2/SO_4^{2-} photocatalyst, Chinese Journal of Catalysis 28 (2007) 528–534.

[9] A.L. Linsebigler, G.Q. Lu, J.T. Yates, Photocatalysis on TiO_2 surfaces: principles, mechanisms, and selected results, Chemical Reviews 95 (1995) 735–758.

[10] J.H. Pan, H.Q. Dou, Z.G. Xiong, C. Xu, J.Z. Ma, X.S. Zhao, Porous photocatalysts for advanced water purifications, Journal of Materials Chemistry 20 (2010) 4512–4528.

[11] W.J. Tseng, P.S. Chao, Synthesis and photocatalysis of TiO_2 hollow spheres by a facile template-implantation route, Ceramics International 39 (2013) 3779–3787.

[12] H. Bala, Y. Yu, Y. Zhang, Synthesis and photocatalytic oxidation properties of titania hollow spheres, Materials Letters 62 (2008) 2070–2073.

[13] Z. Zhong, Y. Yin, B. Gates, Y. Xia, Preparation of mesoscale hollow spheres of TiO_2 and SnO_2 by templating against crystalline arrays of polystyrene beads, Advanced Materials 12 (2000) 206–209.

[14] W.-C. Lin, W.-D. Yang, S.-Y. Jheng, Photocatalytic degradation of dyes in water using porous nanocrystalline titanium dioxide, Journal of the Taiwan Institute of Chemical Engineers 43 (2012) 269–274.

[15] J.Q. Zhao, P. Wan, J. Xiang, T. Tong, L. Dong, Z.N. Gao, X.Y. Shen, H. Tong, Synthesis of highly ordered macro-mesoporous anatase TiO_2 film with high photocatalytic activity, Microporous and Mesoporous Materials 138 (2011) 200–206.

[16] C.Y. Song, W.J. Yu, B. Zhao, H.L. Zhang, C.J. Tang, K.Q. Sun, X.C. Wu, L. Dong, Y. Chen, Efficient fabrication and photocatalytic properties of TiO_2 hollow spheres, Catalysis Communications 10 (2009) 650–654.

[17] X. Sun, J. Liu, Y. Li, Use of carbonaceous polysaccharide microspheres as templates for fabricating metal oxide hollow spheres, Chemistry – A European Journal 12 (2006) 2039–2047.

[18] G.G. Tang, S.S. Liu, H. Tang, D. Zhang, C.S. Li, X.F. Yang, Template-assisted hydrothermal synthesis and photocatalytic activity of novel TiO_2 hollow nanostructures, Ceramics International 39 (2013) 4969–4974.

[19] C. Dwivedi, V. Dutta, Size controlled synthesis and photocatalytic activity of anatase TiO_2 hollow microspheres, Applied Surface Science 258 (2012) 9584–9588.

[20] X.Y. Li, L.H. Chen, Y. Li, J.C. Rooke, C. Wang, Y. Lu, A. Krief, X.Y. Yang, B.L. Su, Self-generated hierarchically porous titania with high surface area: Photocatalytic activity enhancement by macrochannel structure, Journal of Colloid and Interface Science 368 (2012) 128–138.

[21] L.X. Du, Z.T. Jiang, R. Li, Preparation of porous titania microspheres for HPLC packing by sol–gel method, Materials Letters 95 (2013) 17–20.

[22] T. Suntola, Atomic layer epitaxy, Thin Solid Films 216 (1992) 84–89.

[23] R.L. Puurunen, Surface chemistry of atomic layer deposition: A case study for the trimethylaluminum/water process, Journal of Applied Physics 97 (2005) 121301.

[24] S.M. George, Atomic layer deposition: an overview, Chemical Reviews 110 (2010) 111–131.

[25] J. Aarik, A. Aidla, A.-A. Kiisler, T. Uustare, V. Sammelselg, Effect of crystal structure on optical properties of TiO_2 films grown by atomic layer deposition, Thin Solid Films 305 (1997) 270–273.

[26] X.H. Liang, D.M. King, P. Li, A.W. Weimer, Low-temperature atomic layer-deposited TiO_2 films with low photoactivity, Journal of the American Ceramic Society 92 (2009) 649–654.

[27] X.H. Liang, S.M. George, A.W. Weimer, N.H. Li, J.H. Blackson, J.D. Harris, P. Li, Synthesis of a novel porous polymer/ceramic composite material by low-temperature atomic layer deposition, Chemistry of Materials 19 (2007) 5388–5394.

[28] X.H. Liang, L.F. Hakim, G.D. Zhan, J.A. McCormick, S.M. George, A.W. Weimer, J.A. Spencer, K.J. Buechler, J. Blackson, C.J. Wood, J.R. Dorgan, Novel processing to produce polymer/ceramic nanocomposites by atomic layer deposition, Journal of the American Ceramic Society 90 (2007) 57–63.

[29] Y. Ma, Q. Xu, X. Zong, D. Wang, G.P. Wu, X. Wang, C. Li, Photocatalytic H_2 production on $Pt/TiO_2–SO_4^{2-}$ with tuned surface-phase structures: enhancing activity and reducing CO formation, Energy and Environmental Science 5 (2012) 6345–6351.

[30] X.H. Liang, A.W. Weimer, Photoactivity passivation of TiO_2 nanoparticles using molecular layer deposited (MLD) polymer films, Journal of Nanoparticle Research 12 (2010) 135–142.

[31] D.M. King, X.H. Du, A.S. Cavanagh, A.W. Weimer, Quantum confinement in amorphous TiO_2 films studied via atomic layer deposition, Nanotechnology 19 (2008) 445401.

[32] X.H. Liang, A.D. Lynn, D.M. King, S.J. Bryant, A.W. Weimer, Biocompatible interface films deposited within porous polymers by atomic layer deposition (ALD), ACS Applied Materials and Interfaces 1 (2009) 1988–1995.

[33] M.D. Groner, F.H. Fabreguette, J.W. Elam, S.M. George, Low-temperature Al_2O_3 atomic layer deposition, Chemistry of Materials 16 (2004) 639–645.

[34] J.W. Klaus, O. Sneh, S.M. George, Growth of SiO_2 at room temperature with the use of catalyzed sequential half–reactions, Science 278 (1997) 1934–1936.

[35] A.A. Gribb, J.F. Banfield, Particle size effects on transformation kinetics and phase stability in nanocrystalline TiO_2, American Mineralogist 82 (1997) 717–728.

[36] A.R. Liu, S.M. Wang, Y.R. Zhao, Z. Zheng, Low-temperature preparation of nano crystalline TiO_2 photocatalyst with a very large specific surface area, Materials Chemistry and Physics 99 (2006) 131–134.

[37] G. Li, L. Li, J. Boerio-Goates, B.F. Woodfield, High purity anatase TiO_2 nanocrystals: near room-temperature synthesis, grain growth kinetics, and surface hydration chemistry, Journal of the American Chemical Society 127 (2005) 8659–8666.

[38] G. Wang, L. Xu, J. Zhang, T. Yin, D. Han, Enhanced photocatalytic activity of TiO_2 powders (P25) via calcination treatment, International Journal of Photoenergy (2012) 265760.

[39] W.F. Zhang, Y.L. He, M.S. Zhang, Z. Yin, Q. Chen, Raman scattering study on anatase TiO_2 nanocrystals, Journal of Physics D: Applied Physics 33 (2000) 912–916.